

Linear momentum transfer in nonrelativistic nucleus-nucleus collisions

V. E. Viola, Jr.

*Department of Chemistry and Cyclotron Facility, Indiana University,
Bloomington, Indiana 47405*

B. B. Back and K. L. Wolf

Chemistry Division, Argonne National Laboratory, Argonne, Illinois 60439

T. C. Awes and C. K. Gelbke

*Department of Physics and Cyclotron Laboratory, Michigan State University,
East Lansing, Michigan 48824*

H. Breuer

*Department of Physics, University of Maryland,
College Park, Maryland 20742*

(Received 28 December 1981)

The systematic behavior of linear momentum transfer from projectile to target in non-relativistic nucleus-nucleus collisions has been studied using the results of fission-fragment angular-correlation measurements on uranium target nuclei. Data for ${}^4\text{He}$, ${}^{12}\text{C}$, ${}^{16}\text{O}$, and ${}^{20}\text{Ne}$ projectiles have been analyzed over an energy range which extends well above the interaction barrier. The data illustrate the division of the total reaction cross section into two primary components: one associated with ~ 90 percent or greater linear momentum transfer and the other involving much smaller amounts of linear momentum transfer. The former is attributed to fusionlike collisions and the latter to peripheral collisions. The minimum between these two components corresponds to a linear momentum transfer of about 50 percent. It is observed that the ratio of fusionlike collisions to the total reaction cross section decreases regularly as a function of both increasing bombarding energy and projectile mass. From comparison of the experimental fission-fragment angular correlation functions with the predictions of complete fusion kinematics, it is shown that above 10 MeV/nucleon, the experimental definition of complete fusion is complicated by the increasing probability for large, but incomplete, linear momentum transfer collisions. Estimates of critical angular momenta derived from these data do not show any major disagreement with rotating-liquid-drop predictions.

NUCLEAR REACTIONS, FISSION Studied systematics of fission-fragment angular correlation measurements from uranium target nuclei. Deduced linear momentum transfer distributions, fusionlike collision and complete fusion probabilities, and critical angular momenta.

I. INTRODUCTION

A useful overview of the global features of non-relativistic nucleus-nucleus collisions can be obtained from studies of the linear-momentum-transfer distribution which characterizes the target-projectile interaction. For reactions involving highly fissionable target nuclei, where essentially the total reaction cross section is accompanied by fission, information of this type is provided by measurements of the angular correlation between binary fission fragments.¹⁻⁸

As illustrated schematically in Fig. 1, the separation angle between coincident fission fragment pairs, θ_{AB} , serves as an indicator of the linear momentum transferred from the incident projectile to the struck nucleus—thereby contributing to the understanding of the salient mechanisms which describe a given reaction. In the limit of complete linear momentum transfer, processes such as complete fusion yield fission fragments which are emitted with a unique separation angle θ_{AB}° , defined by the momenta of the projectile and the primary fragments. At the opposite extreme, inelastic scattering

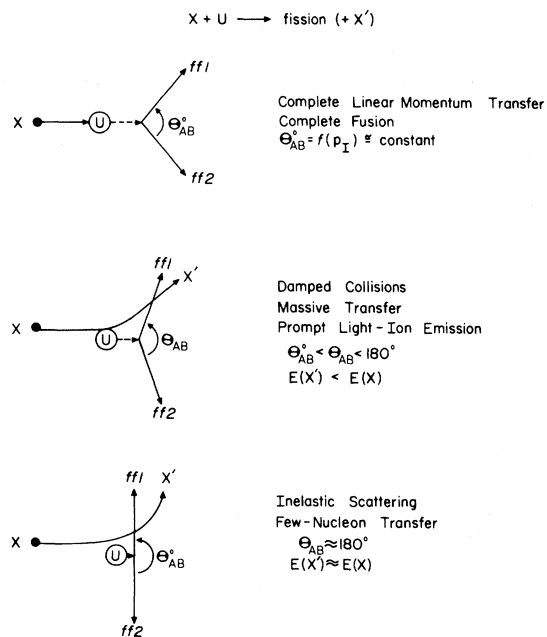


FIG. 1. Schematic diagram of fission fragment opening angles θ_{AB} expected for reaction mechanisms exhibiting widely differing linear momentum transfers.

and few-nucleon transfer reactions impart little momentum to the fissioning nucleus, leading to separation angles near $\theta_{AB} \approx 180^\circ$. Inherent in the quantitative interpretation of such data is the assumption that the fission cross section is equal to the reaction cross section, i.e., excitations of the target nucleus below the fission barrier comprise a negligible fraction of the reaction cross section σ_R .⁶

The fission-fragment angular correlation technique¹ has proven particularly useful in the study of complex-nucleus-induced reaction mechanisms.^{2,3} Nearly twenty years ago it was shown that the reaction cross section in reactions induced by ^{12}C , ^{16}O , and ^{20}Ne projectiles on ^{238}U could be separated into two major components: one corresponding to complete linear momentum transfer and the other to relatively low linear-momentum-transfer processes. These components were originally designated complete fusion (CF) and incomplete fusion (ICF) mechanisms, respectively.³ These and subsequent measurements⁴ demonstrated that the relative importance of complete fusion decreased as a function of increasing projectile mass and also suggested a decrease in σ_{CF}/σ_R as a function of bombarding energy. In subsequent efforts to understand the bombarding-energy dependence using alpha particles⁵⁻⁷ it was shown that at higher energies there exists a continuum of processes in which there is a

strong projectile-target interaction, but in general less than 100 percent linear momentum transfer.

Recently, we investigated the reaction between ^{238}U and ^{16}O ions at 8.75 and 19.7 MeV/nucleon^{8,9} in order to study the evolution of heavy-ion reaction mechanisms as a function of increasing bombarding energy. It is the object of this paper to incorporate these results with those of previous studies in the hope of deriving a more systematic understanding of the distribution of strength of the reaction cross section as bombarding energies increase well above the interaction barrier. In addition, extrapolating these results to higher energies should provide a useful guide for future studies of reactions induced by complex nuclei in the 20 to 100 MeV/nucleon region.

II. FISSION FRAGMENT ANGULAR CORRELATION DATA

The present measurements were performed at the Lawrence Berkeley Laboratory (LBL) 88-inch cyclotron using beams of 140- and 315-MeV ^{16}O ions. The target consisted of 200 $\mu\text{g}/\text{cm}^2$ $^{238}\text{UF}_4$ evaporated onto a 50 $\mu\text{g}/\text{cm}^2$ carbon backing. Coincident fission fragments were detected with a pair of position-sensitive semiconductor detectors placed on each side of the beam at $\pm 80^\circ$ with respect to the beam axis, each subtending an angle of $\pm 18^\circ$ in the reaction plane. Care was taken to perform several redundant measurements to account for target and detector geometry effects. A detailed description of these procedures and the data analysis is given in Refs. 8 and 9.

These results, along with similar data from Refs. 2-7, permit an evaluation of the systematic dependence of linear momentum transfer on projectile mass and bombarding energy. The systems which form the basis for this evaluation are listed in Tables I and II. Selection criteria were (1) the existence of angular correlation measurements at a number of energies extending to above 10 MeV/nucleon; (2) measurements of the entire in-plane, θ , out-of-plane, ϕ , correlation function, for at least one energy for each system; and (3) documented geometries for all measurements. Until recently, the 19.7-MeV/nucleon ^{16}O and 35-MeV/nucleon ^4He data represented the highest E/A beams for which angular correlation measurements on highly fissionable target nuclei were available (in the 10-100 MeV/nucleon range). Experiments have recently been performed at Saturne¹⁰ with 70- and 250-MeV/nucleon ^4He beams and at CERN (Ref.

TABLE I. Ratios of the fusionlike collision cross section σ_F and complete-fusion cross section σ_{CF} to the total reaction cross section σ_R as a function of energy for several complex nucleus reactions with uranium. It is assumed that the fission cross section equals the total reaction cross section in all cases. Also listed are the critical angular momentum for complete fusion, l_{crit}^{CF} and the maximum angular momentum predicted by the rotating-liquid-drop model, l^{RLF} . Both σ_{CF} and l_{crit}^{CF} represent upper limits.

Projectile	Energy/A (MeV/u)	σ_R	σ_F	σ_F/σ_R	σ_{CF}	σ_{CF}/σ_R	l_{crit}^{CF}	l^{RLF}	Reference
${}^4\text{He}$	10.4	1850 ± 60^b	1760^b	0.95 ± 0.05 -0.10	1480	0.80 ± 0.10	18 ± 2	75	2
	12.3	2040 ± 130	1840	0.90 ± 0.05 -0.10	1470	0.72 ± 0.09	20 ± 2	76	5
	17.3	2270 ± 150	1920	0.85 ± 0.08	1380	0.61 ± 0.07	23 ± 2	76	5
	27.5	2300 ± 150	2070	0.90 ± 0.10^a	1495	0.65 ± 0.10^a	28 ± 4	75	6
	35.0	2490 ± 140	2120	0.85 ± 0.10^a	1340	0.54 ± 0.05^a	32 ± 3	76	5
${}^{16}\text{O}$	6.9	923 ± 40^b	831	0.90 ± 0.05	831	0.90 ± 0.05	53 ± 3	69	1
	8.75	1780 ± 70^b	1420	0.80 ± 0.06	1420	0.80 ± 0.06	69 ± 4	69	1,8
	10.4	2130 ± 80^b	1490	0.70 ± 0.05	1410	0.66 ± 0.05	72 ± 4	69	1
	19.7	3590^c	1620	0.45 ± 0.10	1150	0.32 ± 0.07	87 ± 11	69	8
${}^{20}\text{Ne}$	8.75	1900 ± 80	1390	0.73 ± 0.05	1350	0.71 ± 0.05	78 ± 4	68	7
	10.4	2340 ± 90^b	1360	0.58 ± 0.08	1260	0.54 ± 0.08	83 ± 7	68	1
	12.5	2810 ± 140	1350	0.48 ± 0.06	1120	0.40 ± 0.06	85 ± 8	68	7

^aAt 35 MeV/u $\sigma_R(\text{exp})=0.87 \sigma_R(\text{calc})$, where $\sigma_R(\text{calc})$ is derived from a fit of $\sigma_R = \pi x^2 [1 - (V/E)]$ to low-energy data (Ref. 6.). At 27.5 MeV/u these values are $\sigma_R(\text{exp})=0.85 \sigma_R(\text{calc})$; thus $\sigma_F/\sigma_R(\text{calc})=0.77$ and $\sigma_{CF}/\sigma_R(\text{calc})=0.55$.

^bFrom Reference 20.

^cFrom Reference 21.

11) with 56- and 86-MeV/nucleon ${}^{12}\text{C}$ beams. Preliminary results of these investigations will be compared with the results from this analysis in order to infer the macroscopic features of reactions in the 10–100 MeV/nucleon range with similar ions. Although additional angular correlation data exist for ${}^{14}\text{N}$ (Ref. 2) and ${}^{40}\text{Ar}$ (Ref. 12) projectiles, these systems have not been measured over a sufficient energy range to be useful in this study. However, these data are consistent with the results presented here.

In Fig. 2 in-plane angular correlation data for the ${}^{16}\text{O} + {}^{238}\text{U}$ system are shown for several bombarding energies from 110 to 315 MeV (6.9 to 19.7 MeV/u). Figure 3 shows similar data for ${}^{20}\text{Ne} + {}^{235,8}\text{U}$ from 170 to 252 MeV (8.75 to 12.6 MeV/u). In both cases the maximum projectile linear momenta are the same. Except for the lowest ${}^{16}\text{O}$ energy, two components are apparent in the data. At all energies the major fraction of the cross section is concentrated in a well-defined peak corresponding approximately to complete linear momentum transfer. The second component appears at correlation angles slightly smaller than 180° , where one observes the systematic growth of a broad dis-

tribution of relatively low momentum-transfer events.

For each system in Figs. 2 and 3, the arrow indicates the angular correlation centroid angle for complete linear momentum transfer, θ_{AB}° , calculated from kinematics which assumes symmetric mass division and the most probable total kinetic energy release in fission predicted by systematics.¹³ Two factors contribute to the dispersion in the experimental data. The primary source is neutron evaporation before or after fission, which produces an approximately Gaussian spread of the correlation function that is symmetric in θ and ϕ about θ_{AB}° . The width increases with the number of neutrons emitted and can be accounted for quite well by the increase in bombarding energy up to energies of 10 MeV/nucleon. A second source arises from asymmetry in the fragment mass and kinetic energy distributions, which introduces a kinematic dispersion in θ_{AB}° that is skewed toward somewhat lower angles than calculated for symmetry. This factor can serve to decrease θ_{AB}° by about $0.3\text{--}0.6^\circ$ when the entire mass distribution is folded in.^{14,15} For example, in the 315-MeV ${}^{16}\text{O} + {}^{238}\text{U}$ studies, where total

TABLE II. Comparison of experimental centroid angles $\bar{\theta}_{AB}^C(\text{exp})$ for fusionlike collisions with calculated values $\bar{\theta}_{AB}^C(\text{calc})$, based upon symmetric fission of complete fusion system. Values for the centroid shifts, $\Delta\bar{\theta}_{AB}$ represent minimum values, as described in text. Errors in $\% \bar{p}$, are based on uncertainty in $\bar{\theta}_{AB}^C(\text{exp})$.

Projectile	Energy/A (MeV/u)	$\bar{\theta}_{AB}^C(\text{exp})$	$\bar{\theta}_{AB}^C(\text{calc})$	$\Delta\bar{\theta}_{AB}$	$\% \bar{p}$
^4He	10.4	172.5 ± 0.3	172.3	+0.2	98 ± 4
	12.3	172.5 ± 0.2	171.9	+0.6	92 ± 3
	17.3	171.8 ± 0.2	170.8	+1.0	89 ± 3
	27.5	169.8 ± 0.4	168.3	+1.5	87 ± 5
	35.0	168.6 ± 0.2	166.5	+2.1	84 ± 3
^{12}C	6.2	164.3 ± 0.3	164.3	0	100 ± 3
	7.8	162.4 ± 0.3	162.5	-0.1	101 ± 3
	10.4	160.2 ± 0.3	159.9	+0.3	98 ± 3
^{16}O	6.88	158.6 ± 0.3	158.3	+0.3	99 ± 3
	8.75	155.5 ± 0.3	155.8	-0.3	101 ± 3
	10.4	154.6 ± 0.3	154.0	+0.6	98 ± 3
	19.7	147.5 ± 1.0	144.8	+2.7	92 ± 4
^{20}Ne	8.75	153.0 ± 0.2	152.4	+0.6	97 ± 2
	10.4	150.8 ± 0.3	149.8	+1.0	96 ± 3
	12.5	148.7 ± 0.2	146.6	+2.1	93 ± 2

mass and kinetic energy distributions have been determined, a value of $\theta_{AB}^\circ = 144.2$ deg is calculated for the entire fragment distribution, compared with a value of 144.8 deg for symmetric mass division. Since fragment mass and energy distribution data do not exist for all systems studied here, the experimental angular correlation centroids are compared with the value of θ_{AB}° calculated for symmetric mass splits and the most probable total kinetic energy release for the sake of consistency in the systematics. Further, since the width of the mass distribution in uranium fission is not a strong function of excitation energy (FWHM $\simeq 55$ u at 40 MeV of excitation energy compared with ~ 75 u at 280 MeV of excitation energy),⁸ this negative shift in θ_{AB}° remains essentially constant with beam energy over the range of systems studied here. Both nucleon evaporation and fragment mass asymmetry act in such a way as to reduce the sensitivity of the angular correlation technique to the initial dynamics of the target-projectile collision.

The peak associated with large transfers of linear momentum in Figs. 2 and 3 has frequently been attributed to complete fusion. However, because of the dispersive effects of neutron evaporation and

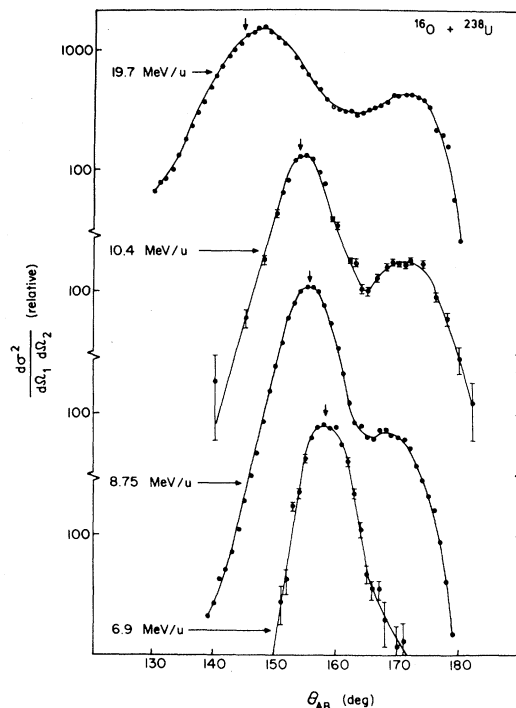


FIG. 2. In-plane angular correlation probabilities for the $^{16}\text{O} + ^{238}\text{U}$ system at energies ranging from 19.7 MeV/u (top) to 6.9 MeV/u (bottom). Data are from Refs. 2, 3, and 8. Arrows indicate expected centroid for complete linear momentum transfer and symmetric mass division.

fragment mass-energy distributions, it is not possible to exclude minor contributions to this peak from high linear-momentum transfer processes such as massive transfer¹⁶ or prompt nucleon emission.⁹ For this reason complete fusion cross sections derived from angular correlation data lack the experimental precision of those determined from evaporation residue studies.¹⁷ (It should be noted that the evaporation residue studies also fail to account for prompt-neutron emission in the entrance channel, thereby also overestimating the complete fusion cross section.) Because of the above effects and uncertainties in the experimental technique, it has previously been estimated that complete fusion cross sections derived from angular-correlation data actually correspond to that part of the cross section involving greater than 95 percent linear-momentum transfer.^{5,6} Consequently, σ_{CF} values determined with this technique must be considered upper limits. By performing an event-by-event analysis of the fragment kinetic energies obtained in angular correlation measurements, it is possible to estimate the

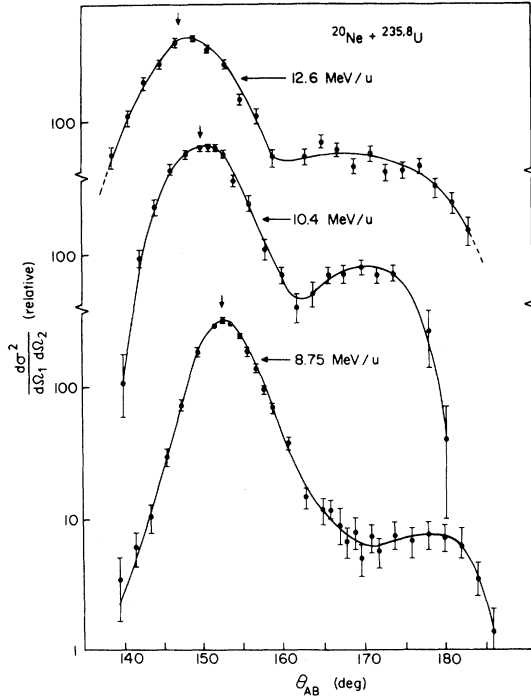


FIG. 3. In-plane angular correlation probabilities for the $^{20}\text{Ne} + ^{235,8}\text{U}$ system at 12.6, 10.4, and 8.75 MeV/u. Data at 12.6 and 8.75 MeV/u are for ^{235}U target; data at 10.4 MeV/u are for ^{238}U target. Data are from Refs. 3 and 4. Arrows indicate expected centroid for complete linear momentum transfer and symmetric mass division.

fragment mass ratio and reduce the uncertainty in momentum transfer from the 5 percent level to 2–3 percent.¹⁵ However, inherent difficulties in these measurements—such as finite detector and target geometry, beam spot size and axial stability, and detector energy and position resolution—prohibit greater accuracy at the present time.

Two systematic features of the angular correlation data in Figs. 2 and 3 stand out. The first of these is the growth of the low-momentum-transfer component with increasing bombarding energy. These events are assumed to be associated with peripheral collisions and we define this component of the cross section as σ_P . In order to evaluate the importance of the peripheral component relative to the total reaction cross section σ_P/σ_R , complete angular correlation data including all out-of-plane events are required. The in-plane data of Figs. 2 and 3 emphasize the probability of events in the reaction plane. However, complete angular correlations as a function of both θ and ϕ demonstrate a large non-planar contribution to peripheral events due to par-

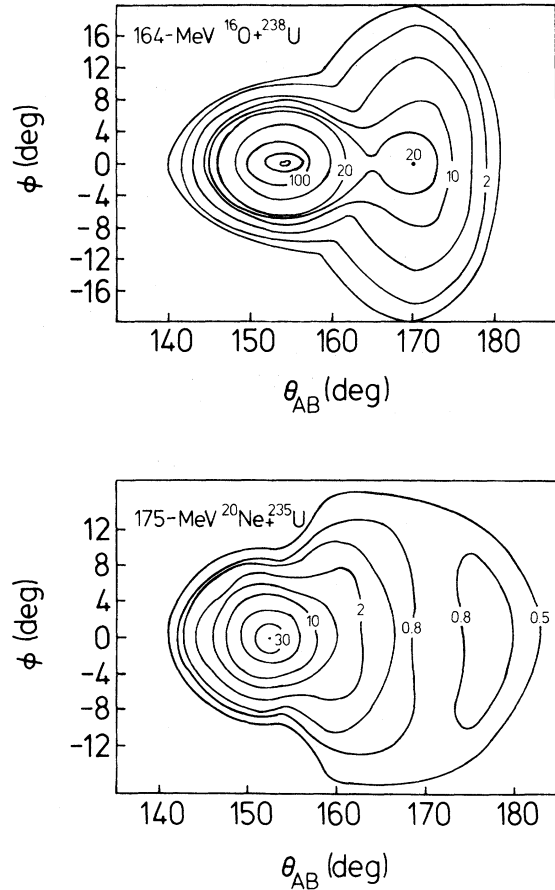


FIG. 4. Probability contours of in-plane angle θ versus out-of-plane angle ϕ for (a) 166-MeV $^{16}\text{O} + ^{238}\text{U}$ and (b) 175-MeV $^{20}\text{Ne} + ^{235}\text{U}$. Data are relative values and are taken from Refs. 3 and 8.

tial momentum-transfer processes. This is illustrated for the 166-MeV $^{16}\text{O} + ^{238}\text{U}$ and 175-MeV $^{20}\text{Ne} + ^{235}\text{U}$ systems in Fig. 4. Complete angular correlations in both θ and ϕ dimensions have been measured for only a few systems; in addition to the above cases these include $^{12}\text{C} + ^{238}\text{U}$ and $^{20}\text{Ne} + ^{238}\text{U}$ at 10.4 MeV/u, $^{20}\text{Ne} + ^{235}\text{U}$ at 12.6 MeV/u, and $^4\text{He} + ^{233}\text{U}$ at all energies listed in Table I. These data indicate that for the full-momentum transfer peak the out-of-plane correlation width is approximately equal to the in-plane width; for peripheral events one observes an increasing width that is approximately related to the momentum of the incident projectile. Based on the systematic behavior of these reactions for which complete measurements have been performed, the in-plane data for other systems have been corrected to account for the unmeasured out-of-plane fraction of the reaction cross section. These corrections are

believed to be accurate to less than ± 0.08 for the ratio σ_P/σ_R .

The low momentum-transfer component of the reaction cross section can best be described in terms of peripheral reactions involving a significant target-projectile interaction during the collision stage in which only a part of the projectile is absorbed. Figure 5 shows angular correlation data for the 315-MeV $^{16}\text{O} + ^{238}\text{U}$ system in which projectile-like and lighter fragments have been observed in coincidence with correlated fission fragments. These data show that Be-O fragments are strongly associated with the peripheral portion of the reaction cross section, presumably associated with nucleon transfer, projectile breakup, and damped reaction mechanisms. Further, it is noted that the mass of the projectile residue appears to decrease as the linear momentum transfer increases. This suggests that at least a fraction of the missing projectile mass has been transferred to the target nucleus. In contrast, the proton- and alpha-particle-gated correlations appear to consist of two components: one related to peripheral processes associated with breakup of excited projectilelike fragments, and the other correlated with the large momentum-transfer component. This latter point will be discussed below.

A second systematic feature of the data in Figs. 2

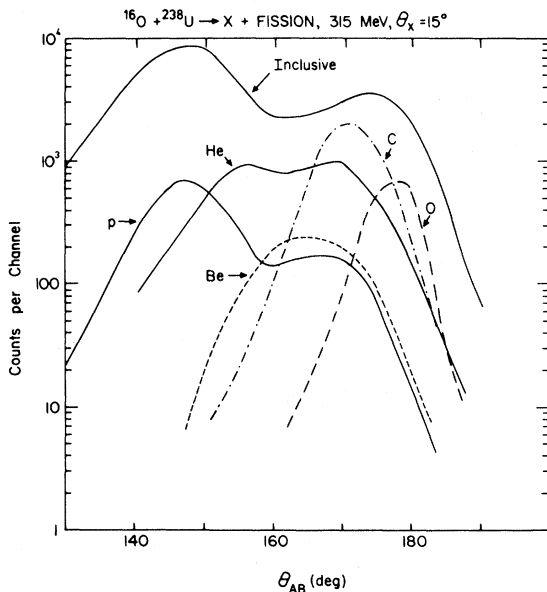


FIG. 5. Angular correlation functions for reactions associated with a third fragment. The inclusive curve includes all events. Lower curves are for protons, alpha particles, Be, C, and O ions in coincidence with fission fragments, as labeled.

and 3 is the energy dependence of the deviation between the calculated centroid for complete momentum transfer and the experimental centroid for this component of the distribution. This deviation, $\Delta\theta_{AB}^\circ$, increases as a function of projectile energy/nucleon and is tabulated in Table II for several systems. It is emphasized that the quoted values of $\Delta\theta_{AB}^\circ$ are lower limits due to the omission of the mass/energy asymmetry factor in the calculated value of θ_{AB}° . Also given in Table II are values of the percentage linear-momentum transfer, $\% \vec{p}$, defined in terms of the ratio of the observed linear-momentum transfer to the beam momentum, $\% \vec{p} = 100p_{\text{exp}}/p_I$. The results below 10 MeV/nucleon based on this centroid analysis are consistent with complete momentum transfer within the previously mentioned accuracy of the technique, which would not be sensitive to massive transfer or prompt nucleon emission processes at the ≤ 10 percent level. For projectile energies above 10 MeV/nucleon it is apparent that on the average, complete momentum transfer becomes increasingly less probable. In addition, as the beam energy/nucleon increases, the fraction of linear momentum transfer decreases systematically. This "missing momentum" has been shown⁹ to be carried off by promptly-emitted light ions, as illustrated by the proton and alpha-particle yields associated with the high momentum-transfer peak in Fig. 5.

From these results it is clear that above 10 MeV/nucleon, and perhaps even lower as argued in Ref. 15, the experimental definition of the complete fusion mechanism is complicated by these large, but incomplete, linear momentum transfer processes. For this reason we propose the term fusionlike collisions for discussing these large momentum transfer events. This terminology is intended to imply capture of a large fraction of the projectile by the target and that these events are produced in low impact-parameter collisions. This definition is intended to be self-consistent with the term central collisions in relativistic heavy-ion collisions, which presumably represent a similar range of impact parameters but lead to more complex final states such as fragmentation. If the fusionlike component is described by a Gaussian, one finds experimentally that these collisions correspond to momentum transfers greater than about $p_{\text{exp}}/p_I \geq 0.5$ and the peripheral collisions to lower values. The data of Fig. 5 demonstrate this approximate separation of mechanisms.

Until very recently the only complex projectiles available for studies of this type at higher energies

have been alpha particles. In Tables I and II and Fig. 6, the angular correlation data for the ${}^4\text{He} + {}^{233,8}\text{U}$ system between 10.4 and 35.0 MeV/nucleon are presented. These show essentially the same features as with the heavier ${}^{12}\text{C}-{}^{20}\text{Ne}$ -induced reactions; i.e., a growth in the fraction of peripheral events and an increasing deviation between calculated and experimental θ_{AB}° values with increasing ${}^4\text{He}$ energy. Unlike the heavier-ion data, the separation between fusionlike and peripheral components is not well-defined due to the relatively low alpha-particle momenta involved. However, the results imply that there is a broad continuum of linear momentum transfers ranging from complete absorption of the alpha particle to inelastic scattering to low-lying states of excitation.^{5,6} This interpretation has been confirmed by studies of light-ion singles spectra¹⁸ which reflect those continuum features, and more recently by fission-fission-light-ion coincidence studies¹⁹ which clearly demonstrate the absorptive-breakup mechanism in which a proton, deuteron, or triton is captured and the remaining projectile fragment is emitted with a distribution of energies centered around the beam E/A . Evidence is also present in these data¹⁹ for prompt proton emission associated with central collisions,

as is observed for the 19.7-MeV/nucleon ${}^{16}\text{O} + {}^{238}\text{U}$ system.⁹ If one takes the percentage of complete-linear momentum transfer $\% \vec{p}$ from Table II as a gauge of these prompt light-ion-emission processes, it is found that their probability scales approximately with the velocity ($\sqrt{E/A}$) of the incident projectile. This behavior is shown in Fig. 7, which suggests that the threshold for such processes occurs somewhere between 8 and 10 MeV/nucleon.

The distribution of strength of fusionlike and peripheral collisions relative to the reaction cross section is summarized in Table I for the data analyzed here. Values for central collision probabilities σ_F were derived by performing a Gaussian fit to the corresponding peak in the angular correlation function. The remaining events were assigned to the probability for peripheral collisions σ_P . Appropriate corrections were made for cases where out-of-plane data did not exist, as discussed above. Values for σ_R were taken from Refs. 2-7, 20, and 21. It is observed that the ratio σ_F/σ_R can be correlated with an effective beam momentum corresponding to an energy E in excess of the Coulomb barrier V , $p_I^{\text{eff}} = \sqrt{2M(E-V)}$. This dependence is shown in Fig. 8(b). Extrapolation of the results for σ_F/σ_R in Table I leads to the conclusion that the

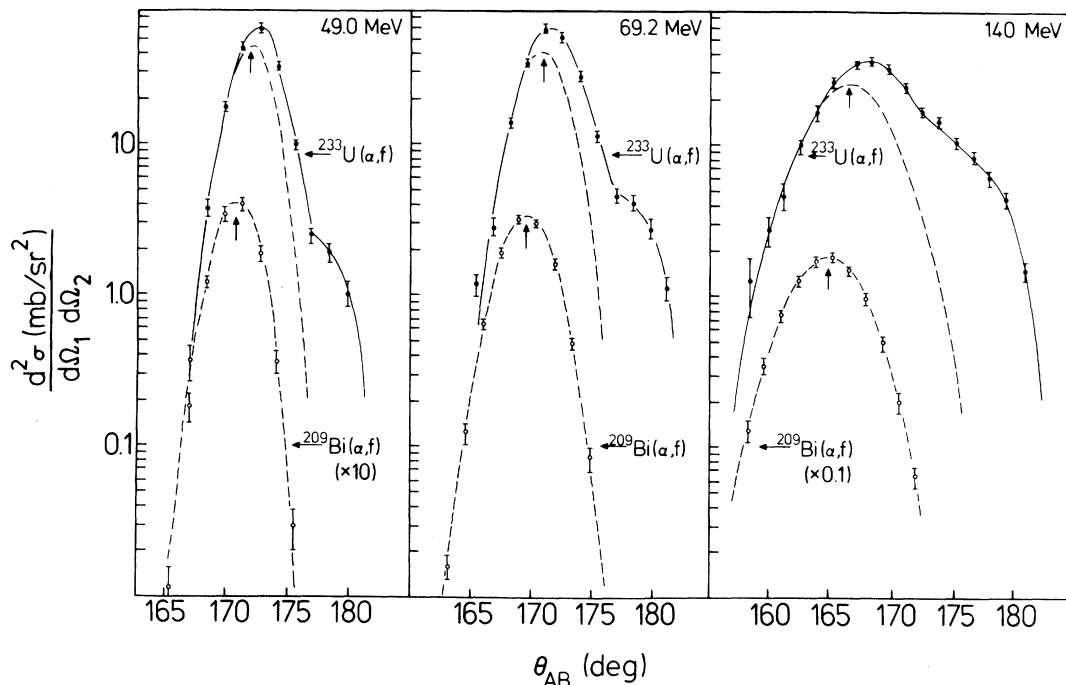


FIG. 6. Total angular correlation functions projected onto the θ axis for reactions of 49.0-, 69.2-, and 140-MeV ${}^4\text{He}$ ions with ${}^{233}\text{U}$. Data are from Ref. 6. Arrows indicate expected centroid for complete linear momentum transfer and symmetric mass division. Dashed line represents complete fusion component as deduced from ${}^{209}\text{Bi} + {}^4\text{He}$ fission under identical conditions.

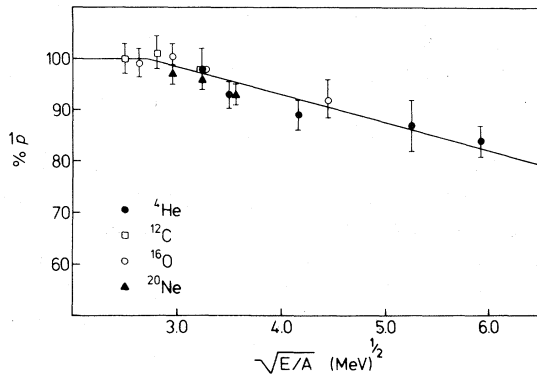


FIG. 7. Plot of percent of full momentum transfer for fusionlike collisions $\% \vec{p}$ as a function of $\sqrt{E/A}$ projectile.

fusionlike component of the cross section for ^{20}Ne and ^{16}O ions should become negligible in the region of 50–70 MeV/u, respectively. For ^4He ions this cutoff is predicted to occur at energies in excess of 100 MeV/u.

Consistent with the systematics of Fig. 8(b), recent results for 70- and 250-MeV/u ^4He ions from Saturne¹⁰ and 56- and 86-MeV/u ^{12}C ions from CERN (Ref. 11) show little evidence for a significant complete momentum transfer component at these higher energies. The implication of these results is that somewhere in the region of 50–70

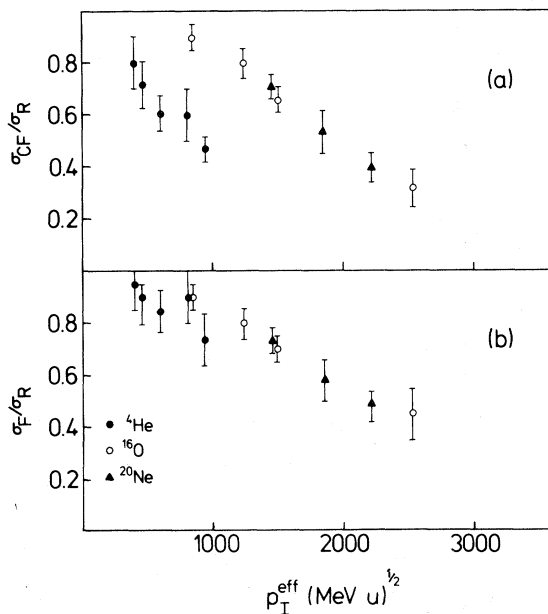


FIG. 8. (a) Plot of the ratio σ_F/σ_R as a function of projectile momentum in excess of the Coulomb barrier p_I^{eff} and (b) plot of the ratio σ_{CF}/σ_R as a function of p_I^{eff} .

MeV/nucleon, the fusionlike component of the reaction cross section no longer can be described in terms of a coherent projectile-target interaction, at least for ^{12}C -to- ^{20}Ne ions. This behavior, coupled with the observation of prompt light-ion emission for 20 MeV/u ^{16}O ions⁹ and 40 MeV/u ^4He ions,¹⁹ suggests that nucleon-nucleon collisions begin to dominate nucleus-nucleus collisions in this energy range at the expense of coherent mean-field processes. The mass dependence of these simple extrapolations implies that for heavier ions, mean-field behavior may disappear at even lower energies.

Although the experimental definition of complete fusion is ambiguous above 10 MeV/u, it is still possible to extract *upper limits* for the complete fusion cross section σ_{CF} for data in this energy range. Values of σ_{CF} for heavy-ion-induced reactions have been derived from these data under the following assumptions: (1) the centroid of the CF angular correlation is given by the calculated θ_{AB}° and (2) the widths of the CF correlation functions increase systematically beyond the low-energy values as predicted by neutron evaporation calculations of the angular dispersion. For the alpha-particle data assumption (2) has been replaced by measurement of the width for $^4\text{He} + ^{209}\text{Bi}$ fission, which is attributed primarily to fission following complete fusion.⁶ It is estimated that inclusion of the mass asymmetry factor in the calculation of θ_{AB}° would lower the values for σ_{CF}/σ_R by ~ 0.05 – 0.10 .

Values for σ_{CF}/σ_R are also listed in Table I and plotted in Fig. 8(a). These are found to decrease even more strongly with bombarding energy than for σ_F/σ_R . Unlike the ratio σ_F/σ_R , for which all the data for ^4He -to- ^{20}Ne projectiles depend systematically on p_I^{eff} , it is not possible to find such a simple parametrization for complete fusion that will account for both the ^4He and ^{12}C -to- ^{20}Ne data. This behavior can most likely be explained as being due to different limitations on the fusion cross section in these two cases, ^4He -induced reactions being limited by the onset of nucleon-nucleon processes, and the heavy-ion-induced reactions being limited by angular momentum effects.

In addition to the implied disappearance of complete fusion at relatively low energies, these results can be used to examine the dependence of the critical angular momentum for complete fusion l_{CF} as a function of bombarding energy. A previous analysis of the $^{20}\text{Ne} + ^{235}\text{U}$ system suggested that the extracted l_{CF} values might violate the rotating liquid drop limit,²² l_{RLD} . However, with the more complete analysis performed here, which accounts

for large but incomplete momentum transfer, it is found that the differences between the experimental upper limit for l_{CF} and the calculated value of l_{RLD} are much smaller. These differences can be reduced even further by the use of more realistic θ_{AB}° values in the derivation of σ_{CF}/σ_F . In addition, the possibility of fission from nonequilibrated systems with shapes outside the fission saddle shape may also explain some of this deviation.²³

III. DISCUSSION

The primary objectives of this analysis have been (1) to summarize the systematic features that characterize nucleus-nucleus reaction cross sections for the experimentally-known region extending well above the interaction barrier and (2) to project these results to energies up to 100-MeV/nucleon range where new accelerator technology will soon make extensive experimental studies possible.

From the results it is apparent that for ^{12}C -to- ^{20}Ne ions at energies of 20 MeV/u and below, the reaction cross section in nucleus-nucleus collisions separates into two distinct components: fusionlike collisions involving complete (or nearly so) linear momentum transfer and peripheral collisions associated with relatively small amounts of linear momentum transfer. The separation between these components occurs at a momentum transfer corresponding to about 50 percent of the beam momentum. Below 10 MeV/nucleon the high linear-momentum-transfer component in these distributions is approximately consistent with a complete fusion mechanism (or full momentum transfer) within the accuracy of the analysis. For higher energies the central-collision peak exhibits a clear trend toward large but incomplete momentum transfer processes. At the highest energies studied here the average central collision momentum transfer is about 85–90 percent of the beam momentum. Since these events are not clearly distinguishable from those involving full momentum transfer, the experimental definition of complete fusion becomes complicated above 10 MeV/u and one must rely on exclusive measurements or model-dependent assumptions to extract complete fusion probabilities from the data.

The missing momentum in the fusionlike component of angular correlations above 10 MeV/nucleon appears to be associated with prompt light-ion emission in the early stages of the target-projectile interaction, as discussed in Ref. 9. Thus, we interpret this feature of the data to be evidence

for the increasing importance of nucleon-nucleon interactions in the entrance channel at the expense of mean-field effects. Consistent with this assumption, we have calculated the linear-momentum-transfer distribution for the $^{238}\text{U} + ^4\text{He}$ system at 140 MeV using a cascade-evaporation code.²⁴ This comparison, shown in Fig. 9, yields a reasonable agreement between theory and experiment. Based on these observations, it is suggested that the mean-field theories generally used for understanding nucleus-nucleus collisions below 10 MeV/

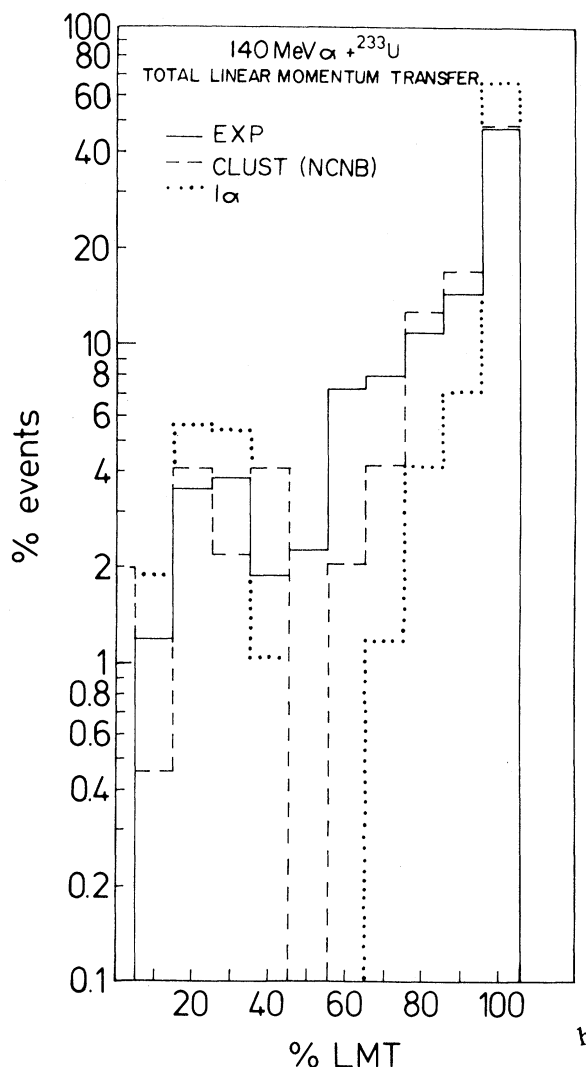


FIG. 9. Comparison of the experimental linear momentum transfer (LMT) distribution for the 140-MeV $^4\text{He} + ^{233}\text{U}$ system (solid line) with calculations based on an intranuclear cascade cluster code. The calculation indicated by the dotted line permits breakup of the incident ^4He ion; the dashed line is for a calculation which does not permit breakup.

nucleon must be modified to include the nucleon-nucleon aspects of the collision at higher energies. This conclusion coincides with the results of DeVries *et al.*, based upon analyses of reaction cross section data.²⁵

Over the energy range studied here it is found that the fusionlike collision cross section remains approximately constant, complete fusion decreases, and peripheral collision probabilities increase as a function of increasing bombarding energy. Similar trends are observed as a function of increasing projectile mass. The implication of these trends is that for light heavy ions, collisions involving large linear momentum transfers should represent a negligible fraction of the reaction cross section by the time energies of 50–70 MeV/nucleon are reached. Complete fusion should disappear at even lower energies. Extrapolating these results to heavier projectiles suggests that limitations on the fusionlike collision cross section due to nucleon-nucleon collision effects will also occur at energies below about 50 MeV/nucleon. However, more extensive data are clearly required to substantiate these estimates.

In conclusion, the present analysis suggests that for projectile energies in the 20–100 MeV/nucleon

region one can expect a wide range of linear momentum transfers to characterize these interactions, leading to a complicated array of final states. Both the sources of prompt light-ion emission and the upper energy limits for well-defined fusionlike collisions represent important problems to be examined in future studies.

ACKNOWLEDGMENTS

The authors wish to thank Dr. W. G. Meyer for many discussions concerning these experiments and early involvement in their planning. Dr. P. Dyer, Dr. A. C. Mignerey, Dr. H. Wieman, and Dr. M. S. Zisman are also acknowledged for their assistance in the early stages of this work. We thank the operating crew at the LBL 88-inch cyclotron for providing the difficult beams for these experiments. One of us (C.K.G.) acknowledges the partial support of the Alfred P. Sloan Foundation and another (V.V.) acknowledges partial support from the John S. Guggenheim Foundation. This work was supported by the U. S. Department of Energy and the National Science Foundation.

¹W. J. Nicholson and I. Halpern, *Phys. Rev.* **116**, 175 (1959).

²T. Sikkeland, E. L. Haines, and V. E. Viola, Jr., *Phys. Rev.* **125**, 1350 (1962).

³T. Sikkeland and V. E. Viola, Jr., *Proceedings of the 3rd Conference on Reactions Between Complex Nuclei* (University of California Press, Berkeley, 1963), p. 232.

⁴V. E. Viola, Jr., R. G. Clark, W. G. Meyer, A. M. Zebelman, and R. G. Sextro, *Nucl. Phys.* **A261**, 174 (1976).

⁵V. E. Viola, Jr., C. T. Roche, W. G. Meyer, and R. G. Clark, *Phys. Rev. C* **10**, 2416 (1974).

⁶W. G. Meyer, V. E. Viola, R. G. Clark, S. M. Read, and R. B. Theus, *Phys. Rev. C* **20**, 1716 (1979).

⁷S. S. Kapoor, H. Baba, and S. G. Thompson, *Phys. Rev.* **149**, 965 (1966).

⁸B. B. Back, K. L. Wolf, A. C. Mignerey, C. K. Gelbke, T. C. Awes, H. Breuer, V. E. Viola, Jr., and P. Dyer, *Phys. Rev. C* **22**, 1927 (1980).

⁹T. C. Awes, G. Poggi, C. K. Gelbke, B. B. Back, B. G. Glagola, H. Breuer, and V. E. Viola, *Phys. Rev. C* **24**, 89 (1981).

¹⁰M. Conjeaud, R. Dayras, S. Harar, H. Oeschler, F. St. Laurent, C. Volant, and J. P. Wieleczko, *Phys. Lett.* **110B**, 372 (1982).

¹¹H. Ho, W. Kühn, U. Lynen, W. F. J. Müller, U. Winkler, D. Pelte, H. Löhner, R. Santo, A. Olmi, Y. T. Chu, P. Doll, A. Gobbi, K. Hildenbrand, and H. Sann,

Gesellschaft für Schwerionenforschung Scientific Report ISSN 0174-0814, 1981, p. 32.

¹²T. Sikkeland, *Phys. Lett.* **27B**, 277 (1968).

¹³V. E. Viola, Jr., *Nucl. Data* **1**, 39 (1966).

¹⁴E. Frick, Ph.D. thesis, University of Maryland, 1975 (unpublished).

¹⁵E. Duek, L. Kowalski, M. Rajagopalan, J. M. Alexander, D. Logan, M. S. Zisman, and M. Kaplan, *Phys. Rev. C* (to be published).

¹⁶D. R. Zolnowski, H. Yamada, S. E. Cala, A. C. Kahler, and T. T. Sugihara, *Phys. Rev. Lett.* **14**, 92 (1978).

¹⁷F. Plasil, R. L. Ferguson, H. C. Britt, B. H. Erkkila, P. D. Goldstone, R. H. Stokes, and H. H. Gutbrod, *Phys. Rev. C* **18**, 2603 (1978); M. N. Namboodiri, E. T. Chulick, J. B. Natowitz, and R. A. Kenefick, *ibid.* **11**, 401 (1975).

¹⁸J. R. Wu, C. C. Chang, and H. D. Holmgren, *Phys. Rev. Lett.* **40**, 1013 (1978); *Phys. Rev. C* **19**, 659 (1979); **19**, 698 (1979).

¹⁹K. K. Kwiatkowski, V. E. Viola, Jr., H. Breuer, C. C. Chang, A. C. Cowley, H. D. Holmgren, and A. C. Mignerey, *Phys. Rev. C* (to be published).

²⁰V. E. Viola, Jr. and T. Sikkeland, *Phys. Rev.* **128**, 767 (1962).

²¹W. Wilcke, J. R. Birkelund, A. D. Hoover, J. R. Huizenga, W. U. Schröder, and H. J. Wollersheim, University of Rochester Report UR-NSRL-221, 1980.

²²S. Cohen, F. Plasil, and W. J. Swiatecki, *Ann. Phys. (N.Y.)* 82, 557 (1974).

²³W. Nörenberg and C. Reidel, *Z. Phys. A* 290, 335 (1979).

²⁴G. J. Mathews, B. G. Glagola, R. Moyle, and V. E. Viola, Jr., *Phys. Rev. C* (to be published).

²⁵N. J. DiGiacomo, R. M. DeVries, and J. C. Peng, *Phys. Rev. Lett.* 45, 527 (1980).